Journal of Materials Science Research; Vol. 5, No. 1; 2016
ISSN 1927-0585 E-ISSN 1927-0593
Published by Canadian Center of Science and Education

Tribological Investigations of PVD Coated Multi-Layer Constructions

Marcus Schulze[1], Holger Seidlitz[1], Franziska König[2] & Sabine Weiß[2]

[1] Chair of Lightweight Construction, Brandenburg University of Technology Cottbus – Senftenberg, Cottbus, Germany

[2] Department of Physical Metallurgy and Materials Technology, Brandenburg University of Technology Cottbus – Senftenberg, Cottbus, Germany

Correspondence: Marcus Schulze, Chair of Lightweight Construction, Brandenburg University of Technology Cottbus – Senftenberg, Cottbus, 03046, Germany. Tel: 490-355-694-625. E-mail: marcus.schulze@b-tu.de

Received: September 23, 2015 Accepted: October 21, 2015 Online Published: December 29, 2015

doi:10.5539/jmsr.v5n1p97 URL: http://dx.doi.org/10.5539/jmsr.v5n1p97

Abstract

Multi-layer constructions become more and more relevant in lightweight applications due to their high strength to weight ratio. They offer excellent crash, damping and recycling properties. Also, the morphology of thermoplastic carbon fibre reinforced plastics (CFRP) render them interesting for large scale manufacturing processes. Nevertheless, a major disadvantage results in a poor resistance against wear and tear, e.g. erosion, which is attributed to weak hardness properties. Hence, this work deals with tribological investigations on orthotropic carbon fibre reinforced polymers (PA 6) either with protective ceramic coating or without. The chosen coating system is a well-known protective covering of metal components, e.g. metal cutting tools, produced by physical vapor deposition (PVD). To characterize the coating system on thermoplastic CFRP, standard analyzing methods are utilized, like optical and scanning electron microscopy (SEM). The tribological investigations are conducted by the tribological ball on disk method to generate wear tracks on the sample surfaces and hence to calculate the wear rates. These results are compared to literature findings with respect to a certain protective coating system (TiN) and a second nano-structured gel coating system, where both systems are deposited on a thermosetting material, i.e. carbon fibre reinforced epoxy resin, respectively. For this purpose the feasibility of depositing a protective ceramic layer on thermoplastic CFRP is demonstrated. First results on suitable surface pre-treatments have shown a significant influence on the coating quality. The improved performance regarding the wear behavior with respect to tribology compared to the poor substrate and existing technologies is shown additionally.

Keywords: thermoplastic composites, protective coating systems, TiAlN – ceramic coating, tribology, wear, physical vapor deposition, scanning electron microscopy

1. Introduction

In the last decade the application of fibre reinforced plastics (FRP) steadily increased in transportation industries. Recent examples are the BMW MegaCity Vehicle Project with the i3 and i8 as well as the BMW i7. For the first time FRP are used in large scale serial production in the automotive industry. In the aerospace industry the Airbus A350 and the Boing 787 have an overall quantity of composite materials of approximately 50 % (Marsh, 2015). Up until now FRP are used for lightweight structures. But increasingly they come into to focus for the application as complex technological systems. For example train couplings in FRP design or hydraulic cylinders manufactured with the filament winding process (Scholz & Kroll, 2014). Polymer coatings are used to enhance the erosion resistance of composite materials (Hertel & Watson, 1996) in aerospace industry. Nevertheless, the life time of such coatings is limited (Tiong & Clark, 2011) and therefore alternative solutions are needed. In a different study the deposition of zinc by pulsed gas dynamic spraying process was used to create wear resistant coatings (Metallic coating of aerospace carbon/epoxy composites by the pulsed gas dynamic spraying process, Surface & Coatings Technology 2009. However the hardness of the zinc coatings is lacking and therefore other solutions are necessary. Other studies have demonstrated the feasibility of the deposition of Ti and TiN layers on CFRP and examined the erosion resistance of these coatings (Maurer & Schulz, 2013, 2014). In this study the feasibility of the application of TiAlN coatings is investigated. TiAlN is one of the most studied hard coating systems. It is used due to its excellent properties such as high hardness, good wear behavior and chemical stability when applied on metal surfaces (Sproul, 1996; PalDey & Deevi, 2003; Jehn, 2000). A lot of former studies examined the deposition of TiAlN on metallic and ceramic substrates (Sveen, Andersson, M'Saoubi, & Olsson, 2013; Ibrahim, Rahmat,

Oskouei, & Singh Raman, 2015; Dobrzański, Pakuła, Křiž, Soković, & Kopač, 2006; Kottfer, Ferdinandy, Hvizdoš & Kaczmarek, 2012). The goal of this work is to prove the possibility to deposit TiAlN hard coatings on FRP and therefore lay the foundation for further investigations into the applications for TiAlN coatings on composite materials. Therefore TiAlN coatings are deposited on thermoplastic composites by means of magnetron sputter deposition. Two different coating thicknesses (s1 = 6 µm, s2 = 20 µm) are prepared. The surface roughness before and after the coating is analyzed. By means of tribological ball on disk tests the coefficient of friction is measured. Scanning electron microscope (SEM) is used to analyze the wear traces.

2. Experimental Setup

2.1 Sample Preparation

To ensure high quality sample surfaces the CFRP specimen (Ø = 30 mm) with a Polyamide 6 matrix and orthotropic reinforced continuous carbon fibres (Table 1) are prepared using a mechanical grinding process with SiC wet sandpapers up to 2500 grit. After the grinding process the samples are cleaned with ethanol. With this pretreatment well prepared sample surfaces are obtained, on which a sufficient coating deposition can be executed. Therefore, the CC 800/9 HPPMs PVD coating machine from CemeCon (Würselen, Germany) is utilized. The conducted coating process is described in detail by (Naveed, Obrosov & Weiß, 2015). In spite of, Figures 1a), 1b) and 1c) give an insight on the possible sample positioning within in the working chamber (Figure 1a)). In addition, Figure 1b) depicts the clamping of the sample and Figure 1c) the directly positioned CFRP sample in front of the combined TiAl-target. The necessary nitrogen to obtain a ceramic TiAlN coating is added in the gaseous state. To compare the influence of varying coating thicknesses among each other, the overall coating time of selected samples has been changed. Therewith, three different coating thicknesses are prepared. A first variation is represented by specimen I with a coating thickness of t = 6 µm. A second variation leads to a coating thickness of t = 20 µm represented by specimen II and III. The third variation regarding specimen III is an additional plasma etching pretreatment prior to the coating deposition. Here, specimen III is pretreated to probably increase the adhesion between TiAlN coating and CFRP surface (Maurer, 2014). Table 2 lists all necessary process parameters regarding the conducted deposition process.

2.2 Measurement of Surface Roughness

The evaluation of the surface roughness allows conclusions regarding the quality of the deposition process as well as the influence of the sample pretreatment. Hence, within the present work detailed investigations on the measurement of the surface roughness value Ra are presented and discussed, respectively. To realize independent conclusions, different measurement techniques were in use, like the Surftest 501 series 178 from Mitutoyo (Illinois, USA), a Keyence VHX-5000 3D microscope (Itasca, USA) and common optical microscopy. Even the influence of the fibre orientation is considered. Therefore Ra is determined parallel as well as perpendicular to the fibres of the top layer. Suitable statistics are generated by conducting a sufficient number of measurements, i.e. 5 points over the surface, with respect to the measurement direction. Finally, the resulting average value (Ra) is calculated and compared among each other.

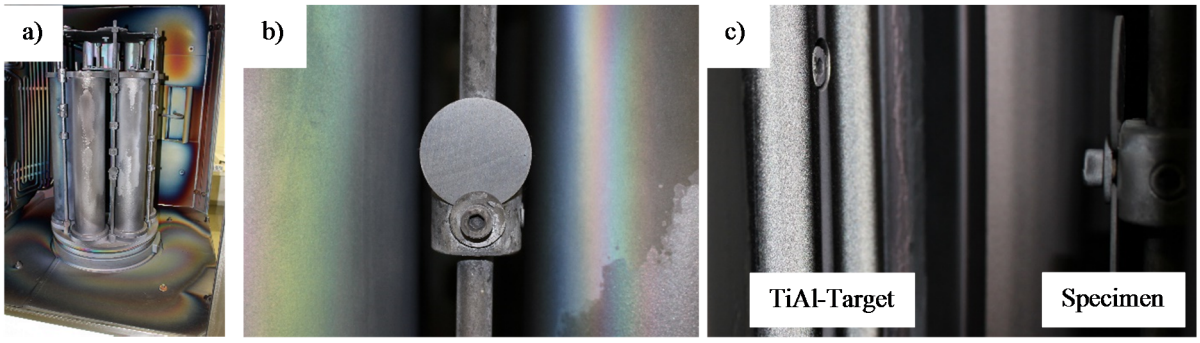

Figure 1. a): Working chamber with specimen holder b): clamping of the sample; c): sample positioned in front of the TiAl – Target

Table 1. Properties of the utilized CFRP

FRP type	Prepreg	Lay up	Young´s modulus $E_1 = E_2$	Tensile strength $\sigma_1 = \sigma_2$	Fibre volume ratio	Thickness	Glass transition temperature
CFRP	UD carbon fibre/PA 6 (Ticona)	$[(0/90)_3]_s$	49.5 GPa	860 MPa	0.6	1.8 mm	220 °C

Note. UD = Unidirectional.

Table 2. Process parameters for deposition process using CC 800/9 HPPMs

Coating process			Unit
Test Chamber	Process temperature	150 ± 5	°C
	Working pressure	< 8.0	mPa
	Argon	200	mln
	Nitrogen	20	mln
Cathode	TiAl Target	2000	W
	Voltage	90	V
	Frequency	280	kHz
Plasma etching pre-treatment			
Argon		160	mln
Table Voltage		650	V
Frequency		240	kHz
Time		300	s

Note. mln = milliliter normal.

2.3 Tribology Testing

To treat the influence of protective coatings deposited on CFRP with respect to the wear and tear behavior in comparison to uncoated CFRP and two other existing coating systems on composites, the tribological ball-on-disc test method is applied (DIN 50324). Therefore, a high temperature tribometer from CSM Instruments (Reseux, Switzerland) is used. In order to realize comparable results the present experimental boundary conditions are in accordance with the investigations of nanocomposite reinforced CFRP (Scholz, Kroll & Schettler, 2014; Scholz & Kroll, 2014). Here, attention should be paid to one limiting condition, which is the material availability. Thus, it was necessary to conduct two tribological tests on each specimen. Consequently, two different working radii (rw = 4 mm; rw = 7 mm) are selected to avoid interferences. Together with the predefined boundary conditions, like wear tracking distance and wear tracking velocity, the tests conducted at a working radius of 4 mm are limited to a certain number of rotations (n = 12,000), which corresponds to a wear tracking distance of 300 m. For the second working radius of 7 mm the limiting requirements result in n = 25,000, which corresponds to a wear tracking distance of 1,100 m, respectively. According to (Scholz, Kroll & Schettler, 2014; Scholz & Kroll, 2014) a load of 10 N is used. The wear partner (counterpart) for all tests is a 100Cr6 steel ball with a diameter of 6 mm applied to the system without lubrication and at room temperature.

3. Results & Discussion

3.1 Coating Quality

The coating quality is an important property, which has to be discussed prior to the evaluation of the surface roughness and the wear behavior. Therefore, all coated samples are investigated by means of optical microscopy (Figure 1). The first results show that on specimen I (Figure 1a)) small cracks along the left side of the sample occur. This peculiarity can be linked to small electric discharges on the sample surface, which were observed at the beginning of the coating process. Larger defects are observed at the surface of specimen II (Figure 1 b)). Here, deformations as well as delaminations took place. Such a delamination was only observed after the start of the coating process. Therefore, it is supposed that low pressure (< 8 mPa) and relatively low temperature (T ≈ 150 °C) boundary conditions in combination with the coating process cause these structural changes. Certain irregularities in the composite matrix and trapped air can be possible reasons as well. The third prepared sample (Figure 1c))

shows merely a small area of delamination on the left side, whereas the remaining specimen surface shows a satisfying structure. At this phase of the work it is particularly noticeable, that all the samples have defects on the left side. This observation can be lessened by the fact, that all specimens were randomly oriented during installation with respect to the fibre orientation of the top layer. Thus, the reason for this defect phenomenon has to be the coating process. Within an industrial coating process multiple targets are used and the sample stage is additionally rotated to improve the coating process quality. In this work, only one TiAl–target was available. Subjected to this condition, a table rotation would have had the consequence of an increased testing time and considerable consumption of the target, respectively. To prevent such a high degradation of the target and for an optimized utilization of the limited conditions, the samples are positioned in static mode right in front of the TiAl- target during the coating process. Besides, a static magnetic field accelerates electrons and Argon ions, wherewith slightly different conditions on the sample surface are generated and possibly produce the observed defects. Nevertheless, all observations regarding the quality of ceramic coating on CFRP confirm the feasibility of protective coatings on composite materials, which will be a great feature in many technical applications.

3.2 Surface Roughness

The surface roughness of either the substrate material or the coated samples has a great influence on the resulting properties. Thus, a suitable surface roughness of the substrate material is decisive for an improved clamping of the deposited protective coating. On the other hand, this positive effect can turn negative, if the surface roughness is too high due to an insufficient bonding between substrate and coating with respect to resulting cavities (Maurer, 2014). It is also necessary to consider, that the utilized PVD deposition process reproduces the surface of the substrate material (Maurer, 2014). This is confirmed by the observations due to optical microscopy. To get first information about the nature of the surface, representative images produced by means of optical microscopy are shown within Figure 2. Here, Figure 2a) depicts the surface morphology of the uncoated and mechanically grinded CFRP substrate. It is peculiar, that the surface shows a rough behavior, i.e. edges and grooves, which are aligned parallel to the top fibre layer. The mechanical pretreatment even exposed the top fibre layer. This rough surface morphology is in accordance with the measured surface roughness values ($Ra,0° = 0.5$ µm; $Ra,90° = 0.7$ µm), which are presented by Figure 3. Here, only a slight deviation occurred with respect to the fibre orientation. Comparable results are discussed within the work of Maurer (Maurer, 2014), who measured the surface roughness of a thermoplastic CFRP, i.e. polyether ether ketone (PEEK), as well. The stated value for the surface roughness is $Ra = 0.4$ µm. As obvious from Figure 3 the surface of specimen I ($t = 6$ µm) is less rough compared to the substrate material, and no corresponding anisotropy with respect to the fibre orientation is observed. This effect is also representative in Figure 1a) and Figure 2a). To get a more detailed insight on the surface morphology a 3D map of the sample surface is generated using a Keyence VHX-5000 3D microscope (Figure 4). Here, the surface irregularities, like grooves and edges, are obvious. Specimen II ($t = 20$ µm), without plasma etching pretreatment, exhibits the highest surface roughness value for the 90° fibre orientation. Note that all measurements are taken in the non-delaminated area. Thus, the high Ra values cannot be explained with the delamination occurred during the coating process. From the literature it is well known, that an increasing coating thickness causes increasing residual stresses within the coating. This may be an explanation for the higher surface roughness. Also the coating growth, which can be different for very thin coatings, can increase the roughness of the coated surfaces. In contrast to these results are the resulting surface roughness values of specimen III (Figure 3). The roughness value Ra is smaller compared to specimen II but with the same coating thickness, and even the fibre orientation has only a slight influence. This can be caused by reduces residual stresses and a more homogeneous coating growth.

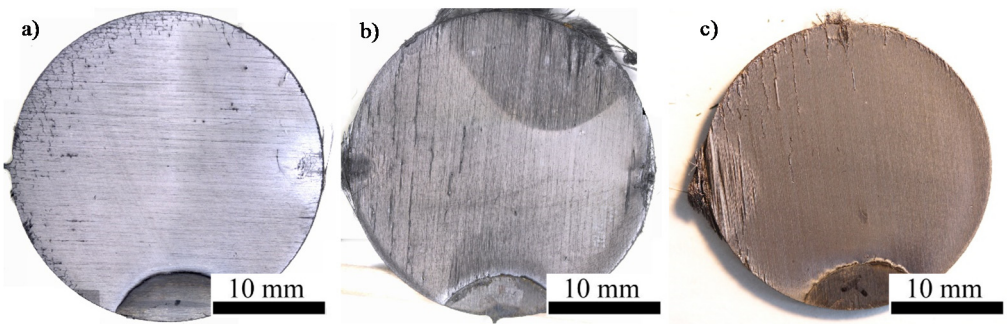

Figure 2. a) specimen I with 6 µm TiAlN layer; b) specimen II with 20 µm TiAlN layer; c) specimen III with 20 µm TiAlN layer with plasma etching pretreatment; d) cross section detail of b

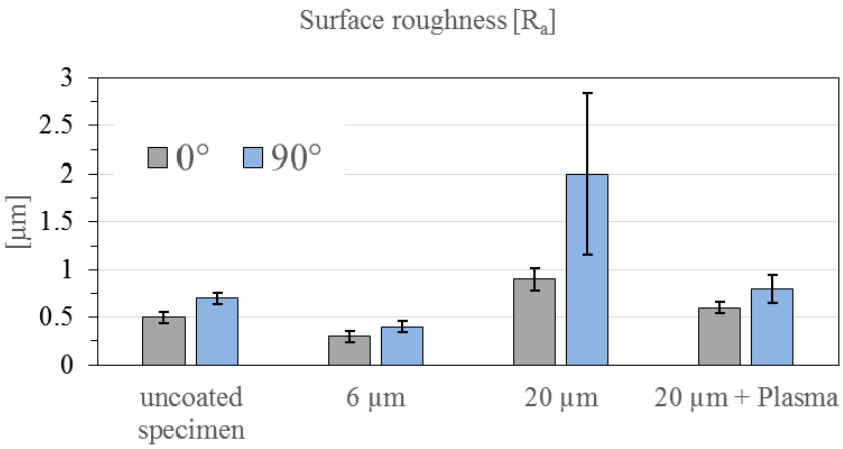

Figure 1. Representation of measured surface roughness values

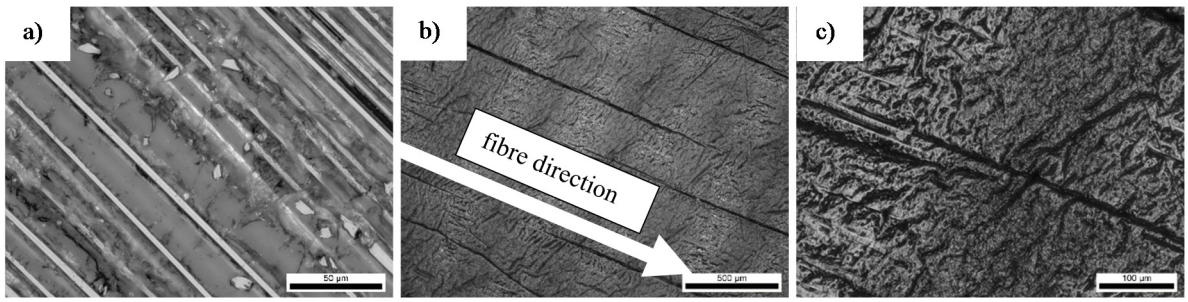

Figure 4. left: Optical microscopic image of an uncoated CFRP specimen produced by mechanical grinding up to 2500 grit; middle: Optical microscopic image of specimen I; right: specimen I with higher magnification

3.3 Tribology Testing

The friction coefficient as a function of the sliding distance is presented in Figure 6. Compared are the specimen I - III and a reference sample without coating (Table 3). The curves exhibit two states, the transient state with a rising coefficient of friction and the steady state with constant or slowly rising friction. From the graphs can be seen, the coating with plasma etching shows a similar friction behavior as the uncoated specimen, albeit at a higher coefficient of friction. Overviews of each wear track and representative detailed magnifications as well an exemplary abrasion of tribological counterpart are given in the Figures 7 - 12.

Specimen I

The first test (normal load 10 N, r_w = 4 mm) aborted before the intended 12000 rotations (300 m sliding distance) could be reached. This was caused by the exceeding of the maximum allowed shear force. The specimen shows an exposure of the substrate material and the fibres in two areas (marked in Figure 7). The damaged areas are at points, where the tribological counterpart moved with 90° to the fibre direction. In areas where the counterpart moved with 0° to the fibre layer, no damage was observed. To avoid the premature termination of the experiments the load is reduced to 5 N for further tests. In the second test (normal load 5 N, r_w = 7 mm) on specimen I, fibre exposure still occurred and the test aborted at 909 m. However, most of the test was completed before termination (909 m of 1100 m). An overview of the wear track is given in Figure 8 and an area of fibre exposure is shown. The area of fibre exposure is drastically reduced, on the whole wear track only a single coating failure is found (Figure 8 middle). At a closer examination the grooves shown in Figure 5 can be seen. The coating failed exactly at one of these groves. Furthermore the parallelism of grooves and fibres is clearly discernible.

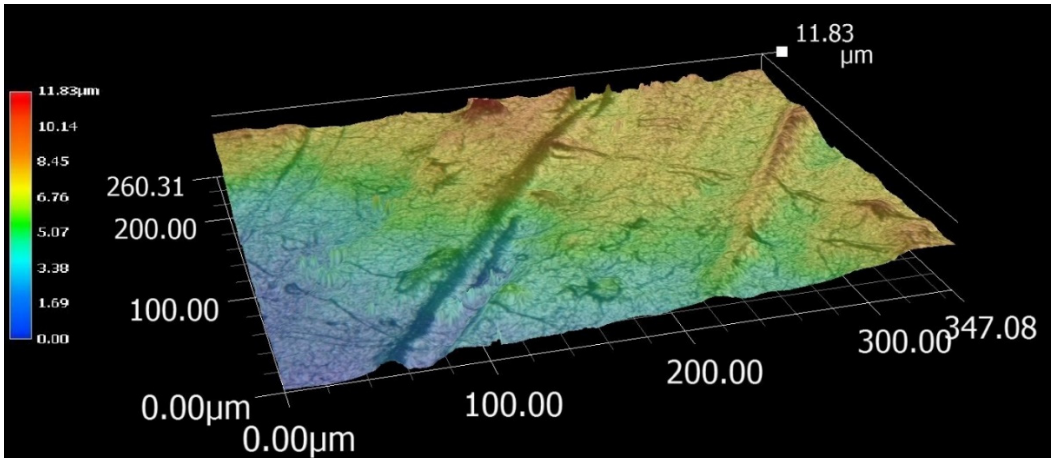

Figure 5. 3D map of the specimen surface with the 6 µm coating (Figure 2a) showing intrusions and extrusions of the TiAlN coating

Specimen II

Specimen II shows no exposure of matrix material or fibres. The test with 4 mm working radius was completed. But the test with 7 mm working radius terminated prematurely similarly to specimen I. The wear of the counterpart in the test with 7 mm working radius is larger than the one with 4 mm working radius, even with a smaller covered distance (Table 3). A possible reason may be the delaminated area (Figure 2b). In this delaminated area the surface roughness is increased and the specimen is no longer flat, but shows a wavy surface. That leads to a greater wear of the counterpart. It should be noted, that even in this delaminated area no fibre exposure occurred. The wear tracks for both test (normal load 5 N, rw = 4 mm & rw = 7 mm) are shown in Figure 9 and 10. On specimen I a difference in the wear could be observed. If the counterpart moved 90° or 0° to the fibre direction. For the 20 µm coating no such effect is observed.

Specimen III

For specimen III both tests (normal load 5 N, rw = 4 mm & rw = 7 mm) where completed. Figure 11 and 12 show the two tribological tests, no exposure of fibres or matrix material was found.

In all tests the wear of the counterpart was conspicuously high. A hardness of 849 ± 29 HV 0.025 for the 100Cr6 balls was measured using micro hardness testing with a load of 25 g. Because of the much higher wear rate of the balls compared to the one of the coating it can be assumed that the deposited TiAlN coating is harder than the 100Cr6 balls. In Figure 13 are given the wear tracks of an uncoated specimen. In the upper part of the wear tracks the deformed matrix material can be seen. Furthermore fibre damage can be observed. In comparison to the results of the coated specimen this shows the suitability of the TiAlN system for the application as a wear resistant coatings. With a high coefficient of friction a higher wear can be expected. When comparing the results of the tests with rw = 4 mm of the specimen II and III, which both are subjected to the same sliding distance and load. A considerable smaller wear was observed on the counterpart of the specimen with the smaller coefficient of friction. The same can be observed in the results of for the tests with rw = 7 mm for specimen I and III. Specimen I shows a higher coefficient of friction and, even with a smaller sliding distance, a greater wear of the counterpart (Figure 6, Table 3).

Table 3. Diameter of Abrasion of tribological counterpart

specimen	Radius r_w [mm]	Load [N]	rotations	Sliding distance [m]	Diameter abrasion 100Cr6 balls [µm]	test
I – 6 µm coating	4	10	7569	190	1470.98	Aborted
	7	**5**	**20 560**	**909**	**1764.57**	**Aborted**
II – 20 µm coating	**4**	**5**	**12 013**	**302**	**1463.87**	**Finished**
	7	5	4247	187	1851.94	Aborted
III – 20 µm coating with plasma etching	**4**	**5**	**12 018**	**302**	**1181.46**	**Finished**
	7	**5**	**25 012**	**1113**	**1673.14**	**Finished**

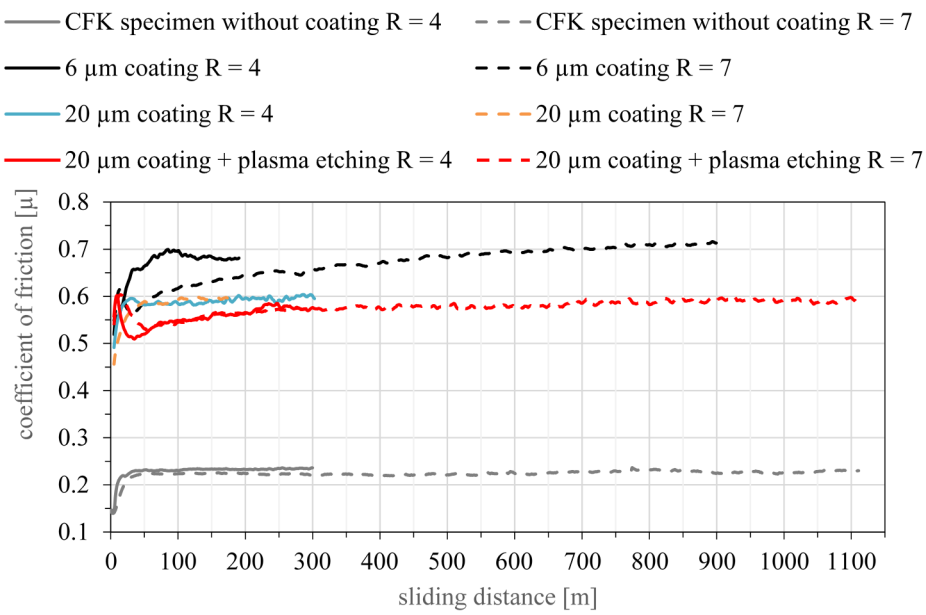

Figure 6. Friction coefficient plotted in relation to the sliding distance

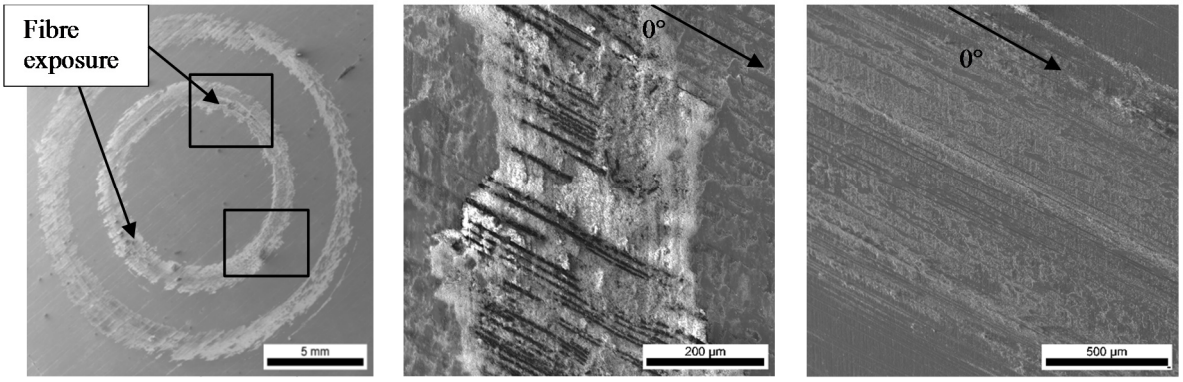

Figure 7. left: overview of Specimen I r_w = 4 mm, middle: exposed fibres, right: undamaged coating

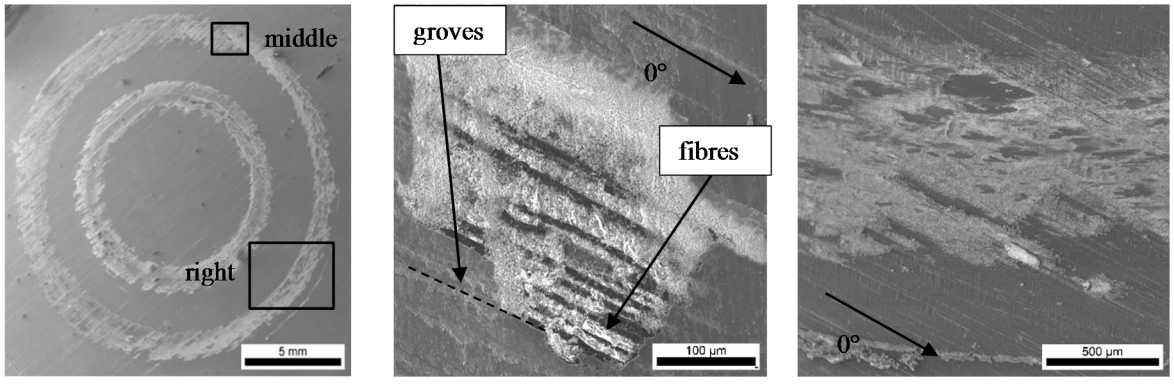

Figure 8. left: overview of Specimen I r_w = 7 mm, middle: exposed fibres, right: undamaged coating

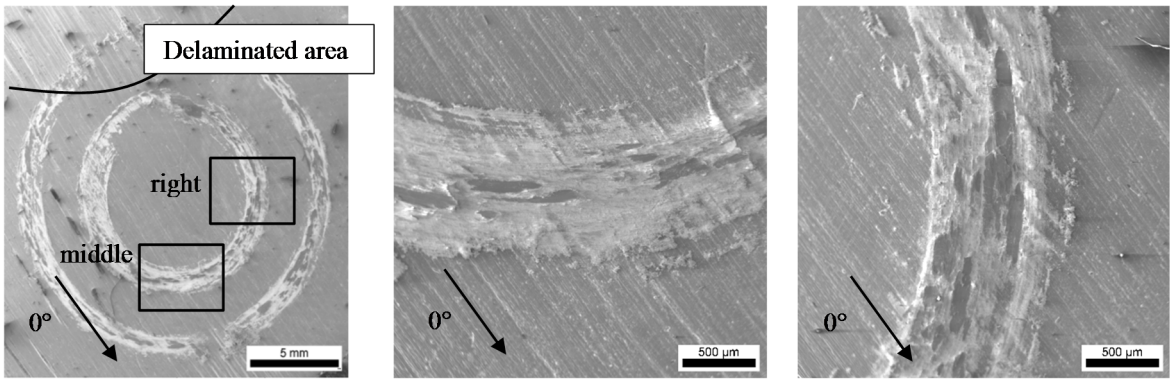

Figure 9. left: overview of Specimen I r_w = 4 mm with delaminated area, middle: undamaged coating, right: undamaged coating

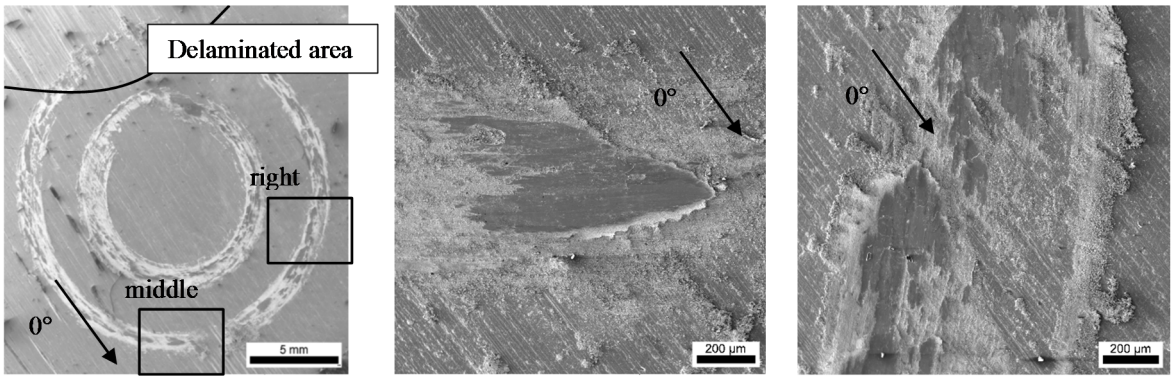

Figure 10. left: overview of Specimen II r_w = 7 mm with delaminated area, middle: undamaged coating, right: undamaged coating

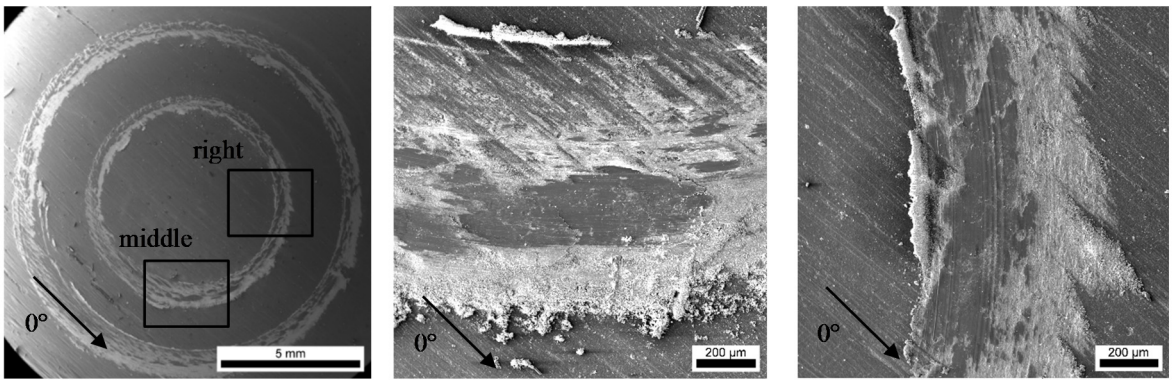

Figure 11. left: overview of Specimen III r_w = 4 mm, middle: undamaged coating, right: undamaged coating

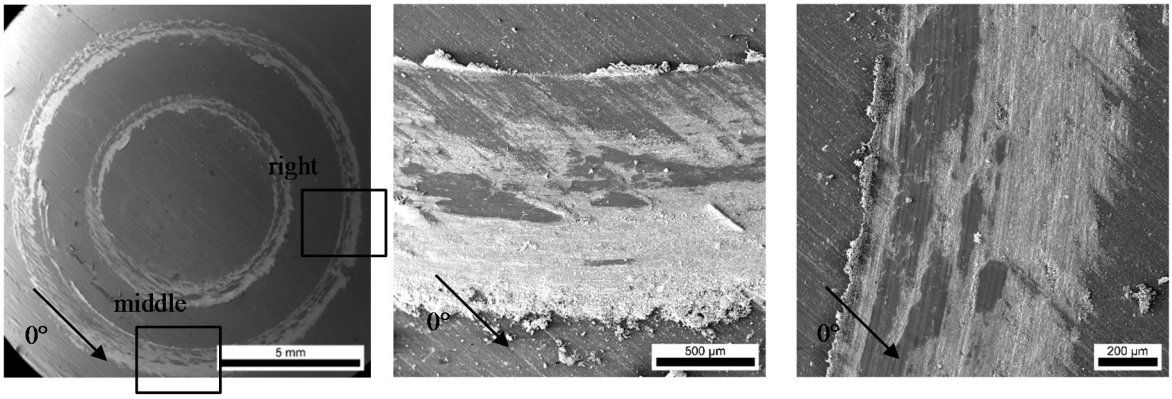

Figure 12. left: overview of Specimen III r_w = 7 mm, middle: undamaged coating, right: undamaged coating

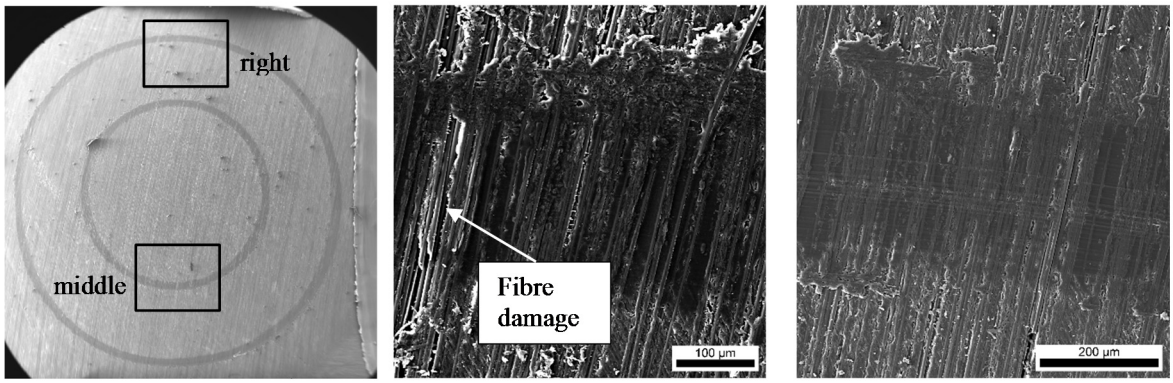

Figure 13. left: overview uncoated specimen, middle: wear track 300 m sliding distance, right: wear track 1100 m sliding distance

4. Conclusions

In this study the deposition of a ceramic TiAlN layer by means of PVD coating process on thermoplastic CRFP is evaluated. The investigations reveal that TiAlN coatings can be applied on CFRP at least up to a coating thickness of t = 20 µm. However, the process parameters have to be improved, to realize high quality protective coating systems, which can be utilized to cover components and parts in many technical applications. Additionally, the presented results show, that a growing coating thickness is directly related to an increase in surface roughness. This effect can be mitigated by applying a suitable plasma etching pretreatment prior to the coating deposition. Nevertheless, further investigations on this topic are necessary. In addition, the presented TiAlN-coating system offer considerable wear resistance compared to uncoated CFRP. This statement is supported due to the absence of discernible effects regarding the conducted tribological investigations for specimen II and III (t = 20 µm). Thus, the presented ceramic coating is well suited for tribological applications, e.g. for substituting sleeves in hydraulic actuators. The wear of the tribological counterpart (849 ± 29 HV 0.025) is considerably higher than that of the coating. Therefore it can be assumed, that the hardness of the coating surpasses that of the counterpart. Here, it has to be considered that hardness testing in areas of thin film technology becomes more complex and has to be treated carefully. From these primary results it is even recommended to utilize ceramic counterparts instead of steel material for further investigations. Since the coating quality is strongly influenced by exposed fibers of the CFRP surface, this has to be treated with great attention. Therefore investigations of applied initial layers, like metallic interface layer, can provide useful results for better adhesion. Future results will be related to these topics.

Acknowledgments

This work was performed within the InnoProfile-Transfer project Lightweight with structured materials, which is supported by the German research foundation BMBF. Financial support is gratefully acknowledged.

References

Dobrzański, L. A., Pakuła, D., Kříž, A., Soković, M. & Kopač, J. (2006). Tribological properties of the PVD and CVD coatings deposited onto the nitride tool ceramics. *Journal of Materials Processing Technology, 175(1-3)*, 179–185. http://dx.doi.org/10.1016/j.jmatprotec.2005.04.032

Hertel, C. J., & Watson, C.R. (1996). Erosion resistant surface protection. *U.S Patent*, Patent Number: US5486096 A

Ibrahim, R. N., Rahmat, M. A., Oskouei, R. H. & Singh Raman, R. K. (2015). Monolayer TiAlN and multilayer TiAlN/CrN PVD coatings as surface modifiers to mitigate fretting fatigue of AISI P20 steel. *Engineering Fracture Mechanics, 137*, 64–78. http://dx.doi.org/10.1016/j.engfracmech.2015.01.009

Jehn, H. A. (2000). Multicomponent and multiphase hard coatings for tribological applications. *Surface and Coatings Technology, 131*(1-3), 433–440. http://dx.doi.org/10.1016/S0257-8972(00)00783-0

Kottfer, D., Ferdinandy, M., Hvizdoš, P., & Kaczmarek, L. (2012). Comperative study of properties of Ti based coatings depositetd by selected PVD techniques.

Marsh, G. (2015). Composites in commercial jets. *Reinforced Plastics, 59*(4), 190-193. http://dx.doi.org/10.1016/j.repl.2015.06.001

Maurer, C., & Schulz, U. (2013). Erosion resistant titanium based PVD coatings on CFRP. *Wear, 302*(1-2), 937–945. http://dx.doi.org/10.1016/j.wear.2013.01.045

Maurer, C., & Schulz, U. (2014). Solid particle erosion of thick PVD coatings on CFRP. *Wear, 317*(1-2), 246–253. http://dx.doi.org/10.1016/j.wear.2014.05.016

Maurer, C. (2014). *Versagensmechanismen von PVD-Beschichtungen auf CFK unter Erosionsverschleiß* (Doctoral dissertation), Rheinisch-Westfälischen Technischen Hochschule Aachen, Germany.

Naveed, M., Obrosov, A., & Weiß, S. (2015). Investigation of the Wear Resistance Properties of Cr/CrN Multilayer Coatings against Sand Erosion. *Conference Papers in Science, 2015*, 1–9. http://dx.doi.org/10.1155/2015/873543

PalDey, S., & Deevi, S. C. (2003). Single layer and multilayer wear resistant coatings of (Ti,Al)N: a review. *Materials Science and Engineering: A, 342*(1-2), 58–79. http://dx.doi.org/10.1016/S0921-5093(02)00259-9

Scholz, S., Kroll, L., & Schettler, F. (2014). Nanoparticle reinforced epoxy gelcoats for fiber-plastic composites under multiple load. *Progress in Organic Coatings, 77*(7), 1129–1136. http://dx.doi.org/10.1016/j.porgcoat.2014.03.012

Scholz, S., & Kroll, L. (2014). Nanocomposite glide surfaces for FRP hydraulic cylinders – Evaluation and test. *Composites Part B: Engineering, 61*, 207–213. http://dx.doi.org/10.1016/j.compositesb.2014.01.044

Sproul, W. D. (1996). Physical vapor deposition tool coatings. *Surface and Coatings Technology, 81*(1), 1–7. http://dx.doi.org/10.1016/0257-8972(95)02616-9

Sveen, S., Andersson, J. M., M'Saoubi, R., & Olsson, M. (2013). Scratch adhesion characteristics of PVD TiAlN deposited on high speed steel, cemented carbide and PCBN substrates. *Wear, 308*(1-2), 133–141. http://dx.doi.org/10.1016/j.wear.2013.08.025

Tiong, U. H., & Clark, G. (2011). Impact of Mechanical Strain Environment on Aircraft Protective Coatings and Corrosion Protection. *Journal of Aircraft, 48*, 1315–1330. http://arc.aiaa.org/doi/abs/10.2514/1.C031270

Woelfle, M. (n.d.). With the A350 XWB Premium AEROTEC pushes in new technological dimensions. Press release.

Copyrights